Catalytic Amplification of the Soft Lithographic Patterning of Si. Nonelectrochemical Orthogonal Fabrication of Photoluminescent Porous Si Pixel Arrays

Yoshiko Harada, Xiuling Li, Paul W. Bohn,* and Ralph G. Nuzzo*

Contribution from the Department of Chemistry and the Frederic Seitz Materials Research Laboratory, University of Illinois at Urbana−Champaign, Urbana, Illinois 61801

Received February 9, 2001

Abstract: Photoluminescent, porous silicon pixel arrays were fabricated via a Pt-promoted wet etching of p-type Si(100) using a 1:1:1 $EtOH/HF/H_2O_2$ solution. The pixels were fabricated with micrometer-scale design rules on a silicon substrate that had been modified with an octadecyltrichlorosilane (OTS) monolayer patterned using microcontact printing. The printed OTS layer serves as an orthogonal resist template for the deposition of a Pt(0) complex, which preferentially deposits metal species in areas not covered with OTS. The Pt centers generate a localized oxidative dissolution process that pits the Si in the Pt-coated regions, resulting in the formation of a porous silicon microstructure that luminesces around 580 nm upon illumination with a UV source. Scanning electron microscopy and fluorescence microscopy images of the fabricated porous silicon structures showed that features in the size range of ∼10−150 μm, and possibly smaller, can be generated by this catalytically amplified soft lithographic patterning method. Importantly, the OTS acts as an etch mask, so that, even with significant hole transport, etching is confined to areas coated with the Pt(0) complex.

Introduction

Porous silicon has been extensively studied since the discovery in 1990 of its efficient luminescence properties at room temperature,[1] following the pioneering work by Ulhir[2] and Turner.[3] The current technological interests in porous silicon focus on the remarkably high surface area, enhanced chemical reactivity, and novel physical properties of this material. Biological[4,5] and chemical[6,7] sensors that operate by detecting changes in Fabry−Perot interference fringes have been fabricated on chemically modified porous silicon thin films. Porous silicon has also shown some promise as a substrate material and trap for analyte molecules in matrix-free desorption/ionization mass spectrometry.[8] The porous silicon serves a dual function in this latter application, acting both as a sample host and as an energy transduction medium for the high-energy laser radiation used to vaporize and ionize the analyte. Because many of the potential applications for porous silicon lie in microelectronics, microoptics, and related fields that require miniaturization, development of an efficient method for micropatterning this material is highly desirable.

The formation of porous silicon is typically accomplished either by anodic etching in HF solution or by stain etching in HF/HNO_3 solution.[9] The structures, and thus the properties, of the porous silicon films generated by these methods depend sensitively both on the substrate type and on the etching conditions used (such as the chemical composition of the etchant and the etch time).[10,11] In stain etching, no external electrochemical bias is required; the holes necessary for sustaining the oxidative dissolution are supplied by the HNO_3 or other strong chemical oxidants. Recent publications describe alternative routes to the formation of porous silicon; in this method, Pt is deposited directly on a Si substrate and acts as a reaction mediator that promotes the wet etching without the need for an external bias. The Pt can be deposited either by plating Pt from a Pt(IV) solution while etching at rest potential in HF[12] or by sputtering the metal onto the substrate prior to etching in HF/H_2O_2 solutions.[13] It is believed that the dissolution of Si is facilitated by hole injection through the Pt ions in the former example or through the reduction of H_2O_2 at the local Pt cathode in the latter. The addition of Pt as a key contributor in the etching process provides an attractive approach for triggering porous silicon formation in selected areas of a sample. Considering the high reactivity of a typical etchant (i.e., HF/oxidizing agent), it is more feasible to introduce a Pt-bearing patterned substrate into the etchant than to simultaneously deposit Pt and etch in the same solution. Luminescent porous silicon films have been fabricated on sputter-coated Pt patterns with feature sizes of >1 mm,[13] but the formation of micrometer-scale patterns has yet to be demonstrated.

* Corresponding author: (e-mail) r-nuzzo@uiuc.edu; (phone) 217-244-0809; fax) 217-244-2278.

(1) Canham, L. T. *Appl. Phys. Lett.* **1990**, *57*, 1046−1048.
(2) Ulhir, A. *Bell Syst. Technol. J.* **1956**, *35*, 333−347.
(3) Turner, D. R. *J. Electrochem. Soc.* **1958**, *105*, 402−408.
(4) Dancil, K.-P. S.; Greiner, D. P.; Sailor, M. J. *J. Am. Chem. Soc.* **1999**, *121*, 7925−7930.
(5) Janshoff, A.; Dancil, K.-P. S.; Steinem, C.; Greiner, D. P.; Lin, V. S.-Y.; Gurtner, C.; Motesharei, K.; Sailor, M. J.; Ghadiri, M. R. *J. Am. Chem. Soc.* **1998**, *120*, 12108−12116.
(6) Létant, S. E.; Sailor, M. J. *Adv. Mater.* **2000**, *12*, 355−359.
(7) Sohn, H.; Létant, S.; Sailor, M. J.; Trogler, W. C. *J. Am. Chem. Soc.* **2000**, *122*, 5399−5400.
(8) Wei, J.; Buriak, J. M.; Siuzdak, G. *Nature* **1999**, *399*, 243−246.
(9) Cullis, A. G.; Canham, L. T.; Calcott, P. D. J. *J. Appl. Phys.* **1997**, *82*, 909−965.
(10) Beale, M. I. J.; Bemjamin, J. D.; Uren, M. J.; Chew, N. G.; Cullis, A. G. *J. Cryst. Growth* **1985**, *73*, 622−636.
(11) Beale, M. I. J.; Benjamin, J. D.; Uren, M. J.; Chew, N. G.; Cullis, A. G. *J. Cryst. Growth* **1986**, *75*, 408−414.
(12) Gorostiza, P.; Diaz, R.; Kulandainathan, M. A.; Sanz, F.; Morante, J. R. *J. Electroanal. Chem.* **1999**, *469*, 48−52.
(13) Li, X.; Bohn, P. W. *Appl. Phys. Lett.* **2000**, *77*, 2572−2574.

10.1021/ja010367j CCC: $20.00 © 2001 American Chemical Society
Published on Web 08/16/2001

Several techniques with the potential for patterning porous silicon with much smaller feature sizes have been described in the literature. These methods include patterning based on photolithography, photoinduced chemical reactions, and ion implantation. Irradiation of a silicon substrate through a projection mask using 450-nm light during anodic etching has been reported to give feature sizes with a lateral resolution of ~20 μm.[14] The resolution achievable with this method is limited by the image spreading that results from carrier diffusion in the Si. Photopatterned porous silicon with feature sizes down to 40 μm has been obtained by chemically functionalizing the porous silicon surface through a photosensitive hydrosilylation of surface silicon hydrides after initial production of porous silicon.[15] Pattern transfer in porous silicon has also been obtained via use of a photoresist mask.[16] The resist pattern in this case was generated on a previously prepared anodic porous silicon film and the pattern then inscribed in the porous silicon film via reactive ion etching (RIE). The limiting lateral resolution achieved by this method was again found to be about several micrometers, being limited largely by the considerable roughness of the porous silicon film. Porous silicon architectures with submicrometer feature sizes have been formed anodically on a substrate masked with a lithographically defined pattern of a suitable etch stop such as silicon nitride.[17] Appreciable etching under the mask and crack formation were encountered, complicating the use of this latter technique, however. Pattern transfer can also be derived from sample damage profiles. In this method, selective ion implantation was used to amorphize specific areas of a single-crystal Si substrate prior to anodic etching; luminescence was obtained only from areas that were not previously amorphized.[18] Doping levels are known to modulate the etching properties of Si, and it has been shown that submicrometer-scale patterns of porous silicon can be obtained by a Ga^+ focused ion beam implantation doping followed by stain etching.[19]

Although the fine patterning of porous silicon microstructures can be achieved with currently available methods, most of them require complex fabrication and thin-film deposition tools, suffer from time-consuming procedures, and are limited by their scalability and process quality variations. It has been shown that soft lithographic patterning methods possess process advantages that can circumvent these concerns for many materials of interest.[20,21] With this motivation, we explored directed chemistries to enable pattern transfer by microcontact printing (μCP), a soft lithographic technique capable of producing submicrometer patterns on silicon[22,23] and other thin-film substrates.[24−26] Monolayer films patterned by μCP have been used in the past as orthogonal resists for directing further modifications. Notably, μCP films have been used as templates in the selective deposition of polymer microstructures[27−29] and the additive chemical vapor deposition of patterned metal thin films.[30,31]

The efficacy of Pt-mediated etching coupled with the intense technological interest in patterning porous semiconductors naturally suggested localized delivery of zerovalent Pt as a strategy for spatially directing the formation of porous silicon. We describe here a method that effectively combines the advantages of a Pt-promoted etching of Si, directed deposition and μCP to create patterned porous silicon on the micrometer-length scale. In our method, μCP is used to pattern octadecyltrichlorosilane (OTS) monolayers on a Si substrate; these OTS structures serve as a passivating resist pattern and ultimately yield porous silicon structures with dimensions that highly complement those produced by the method described by Sailor and co-workers.[14] A Pt(0)−divinyltetramethyldisiloxane complex is selectively deposited orthogonal to the OTS-covered regions (i.e., selectively in non-OTS areas),[32,33] which upon etching with $EtOH/HF/H_2O_2$ generates a localized (and thus patterned) oxidative dissolution of the substrate. The porous silicon microstructures formed in this way are complementary to the OTS pattern. In this paper, we describe how the μCP-directed chemical etching is implemented, the physical characterization of the porous silicon microstructures generated by it, and the templates used in fabricating them.

Experimental Section

B-Doped, p-type Si(100) wafers (Silicon Sense, test grade, 1−25 Ω cm) cut into ~1 × 1 cm^2 pieces were rinsed with deionized water (DI), acetone, and 2-propanol (IPA) and dried in a nitrogen stream. The wafers were placed in a UV/ozone chamber for at least 15 min, rinsed with DI, and then dried in a stream of nitrogen. A 10 mM OTS (Gelest) solution was prepared using toluene as a solvent. The OTS ink was coated on a poly(dimethylsiloxane) (PDMS) stamp using a photoresist spinner (3000 rpm for 30 s) and dried in a stream of nitrogen for 30 s. The stamp was manually placed on a clean Si substrate for 3−5 min at 45 °C. The stamp was removed from the substrate, rinsed with IPA, and dried with nitrogen. The substrate was rinsed with IPA and DI and dried with nitrogen. This procedure yielded an OTS film thickness of ~22 Å as determined by ellipsometry. The OTS patterned substrate was annealed at 70 °C for 1 h in a drying oven and then was coated twice by spin-coating with a ~0.3 mM Pt(0)−divinyltetramethyldisiloxane (2.1−2.4% in xylene, Gelest) solution diluted in toluene, using the same conditions described above. The substrate was annealed at 70 °C for 1 h in a drying oven, rinsed with IPA and DI, and dried in a nitrogen stream.

The samples were etched either by placing a 50-μL drop of etchant on the substrate or by immersing the substrate in the etchant composed of 1:1:1 v/v/v EtOH, 49% HF (Fisher), and 30% H_2O_2 (Fisher). The etch times used (see below) varied between 10 s and 5 min. Etched samples were rinsed with DI and dried in a stream of nitrogen.

(14) Doan, V. V.; Sailor, M. J. *Appl. Phys. Lett.* **1992**, *60*, 619−620.
(15) Stewart, M. P.; Buriak, J. M. *Angew. Chem., Int. Ed. Engl.* **1998**, *37*, 3257−3260.
(16) Couillard, J. G.; Craighead, H. G. *J. Vac. Sci. Technol. B* **1994**, *12*, 161−162.
(17) Nassiopoulos, A. G.; Grigoropoulos, S.; Canham, L.; Halimaoui, A.; Berbezier, I.; Gogolides, E.; Papadimitriou, D. *Thin Solid Films* **1995**, *255*, 329−333.
(18) Bao, X.-M.; Yang, H.-Q. *Appl. Phys. Lett.* **1993**, *63*, 2246−2247.
(19) Steckl, A. J.; Xu, J.; Mogul, H. C.; Mogren, S. *Appl. Phys. Lett.* **1993**, *62*, 1982−1984.
(20) Zhao, X.-M.; Xia, Y.; Whitesides, G. M. *J. Mater. Chem.* **1997**, *7*, 1069−1074.
(21) Xia, Y.; Whitesides, G. M. *Angew. Chem., Int. Ed. Engl.* **1998**, *37*, 550−575.
(22) Wang, D.; Thomas, S. G.; Wang, K. L.; Xia, Y.; Whitesides, G. M. *Appl. Phys. Lett.* **1997**, *70*, 1593−1595.
(23) Zhong, Z.; Gates, B.; Xia, Y.; Qin, D. *Langmuir* **2000**, *16*, 10369−10375.
(24) Kumar, A.; Biebuyck, H. A.; Whitesides, G. M. *Langmuir* **1994**, *10*, 1498−1511.
(25) Xia, Y.; Kim, E.; Mrksich, M.; Whitesides, G. M. *Chem. Mater.* **1996**, *8*, 601−603.
(26) Kind, H.; Geissler, M.; Schmid, H.; Michel, B.; Kern, K.; Delamarche, E. *Langmuir* **2000**, *16*, 6367−6373.
(27) Xia, Y.; Mrksich, M.; Kim, E.; Whitesides, G. M. *J. Am. Chem. Soc.* **1995**, *117*, 9576−9577.
(28) Huang, Z.; Wang, P.-C.; MacDiarmid, A. G.; Xia, Y.; Whitesides, G. *Langmuir* **1997**, *13*, 6480−6484.
(29) Huck, W. T. S.; Yan, L.; Stroock, A.; Haag, R.; Whitesides, G. M. *Langmuir* **1999**, *15*, 6862−6867.
(30) Jeon, N. L.; Clem, P. G.; Payne, D. A.; Nuzzo, R. G. *Langmuir* **1996**, *12*, 5350−5355.
(31) Jeon, N. L.; Lin, W.; Erhardt, M. K.; Girolami, G. S.; Nuzzo, R. G. *Langmuir* **1997**, *13*, 3833−3838.
(32) Laibinis, P. E.; Hickman, J. J.; Wrighton, M. S.; Whitesides, G. M. *Science* **1989**, *245*, 845−847.
(33) Hickman, J. J.; Laibinis, P. E.; Auerbach, D. I.; Zou, C.; Gardner, T. J.; Whitesides, G. M.; Wrighton, M. S. *Langmuir* **1992**, *8*, 357−359.

Optical micrographs were recorded with a Carl Zeiss SV11 dissecting microscope equipped with a color CCD camera (NEC, model NX18AS) and an Olympus BH-2 microscope equipped with a color CCD camera (Panasonic, model GP-KR222). Photoluminescence spectra were recorded on a SPEX fluorometer equipped with a 500-W Xe lamp, two monochromators, and a Hamamatsu RT220P PMT. The samples were etched and placed in the sample holder immediately before collecting data. Fluorescence microscope images were recorded using an inverted microscope (Zeiss Axiovert 100) equipped with a 150-W Hg lamp and a color camera (Sony Medical Instruments, model DCX 9000). Scanning electron microscopy (SEM) images were obtained using a high-resolution field emission SEM (Hitachi S4700) to study the surface morphology. The accelerating voltage used was 10 kV. To prevent charging in the etched Si regions, the samples were first coated with a thin gold layer (less than 10 nm) using standard methods prior to analysis. The surface chemical compositions of the unpatterned samples were determined using X-ray photoelectron spectroscopy (XPS) on a Physical Electronics PHI 5400 spectrometer using a monochromatic Al Kα source (15 kV, 500 W). The survey scans were collected at a constant pass energy of 178.95 eV, and the multiplex scans were collected at 35.75 eV. All samples were analyzed at a 45° tilt angle. Parallel imaging mode XPS data were acquired on a Kratos AXIS Ultra spectrometer using a monochromatic Al Kα source (15 kV, 225 W) with the neutralizer on. The images were collected at a constant pass energy of 160 eV. All images were recorded at a 90° angle relative to the surface of the sample and with the minimum iris size of ~2.5 mm. Pt and C images were collected at 74 and 285 eV, respectively. Both were corrected for charging and background noise. Scanning Auger electron spectroscopy data were obtained on a Physical Electronics PHI 660 scanning Auger microprobe operated at 10 keV. Dynamic secondary ion mass spectrometry (SIMS) images were recorded on a Cameca IMS 5f spectrometer. A Cs^+ (14.5 keV, 22 nA/cm^2) source was used as the primary ion beam.

Results

Fabrication of Soft Lithographically Patterned Porous Silicon Layers and Characterization by Optical Microscopy. The general procedure used to fabricate patterned porous silicon microstructures is summarized in Scheme 1. The p-type Si(100) wafers used as substrates were first modified with patterned monolayers of OTS by μCP. The ink used to print these layers was a 10 mM solution of OTS in toluene, and during the printing, the sample was held at 45 °C. Our typical stamp for the printed OTS pattern consisted of circular holes of ~150-μm diameter and crosses formed by two intersecting channels ~10 μm wide × 40 μm long. The structure of this stamp is illustrated by a micrograph that shows a section of the PDMS stamp used to prepare the patterned OTS layers (Supporting Information). Following the printing step, the samples were annealed at 70 °C for 1 h to improve their substrate adhesion and barrier properties.[34] A dilute solution of a Pt(0)−divinyltetramethyldisiloxane catalyst in toluene was coated on the sample by two successive spin-casting applications. The treated sample was then heated at 70 °C for 1 h to remove the remaining solvent and form Pt colloids in the non-OTS-bearing regions (see below).[35] Without the annealing step, the Pt complex was removed when the sample was rinsed with 2-propanol and deionized water. At the Pt(0) complex concentrations used here, this treatment did not degrade the appearance of Si(100) wafer; higher concentrations, though, resulted in the formation of visible aggregates. The Pt-coated samples were etched using a solution composed of 1:1:1 EtOH/HF (49%)/H_2O_2 (30%) by volume. The wetting properties of the OTS resist strongly influence the etching. For example, a single drop of the etchant solution generates pixels bounded by a discrete contact line (image shown in Supporting Information). A similar drop of etchant spreads to cover the entire ~1 × 1 cm^2 surface of a substrate without the OTS pattern. The rate of spreading is small enough on a patterned sample to restrict the etching largely to those regions residing within the diameter of the drop.

The optical micrographs shown in Figure 1 demonstrate the time dependence of this etching. As etching time increases, the patterned dots change color—from gray to brown, to blue, to green, to yellow, to brown, etc. The etching process is most evident initially at or near the center of each pixel, extending outward in a radial fashion for longer etch times. For substrates without the Pt coating, treatment with the same etchant in this way induced no color change. Similarly, when the substrate was printed with an unpatterned OTS monolayer, and subsequently coated with Pt, there was no color change seen upon etching

Scheme 1. General Procedure for Patterned Porous Silicon Fabrication[a]

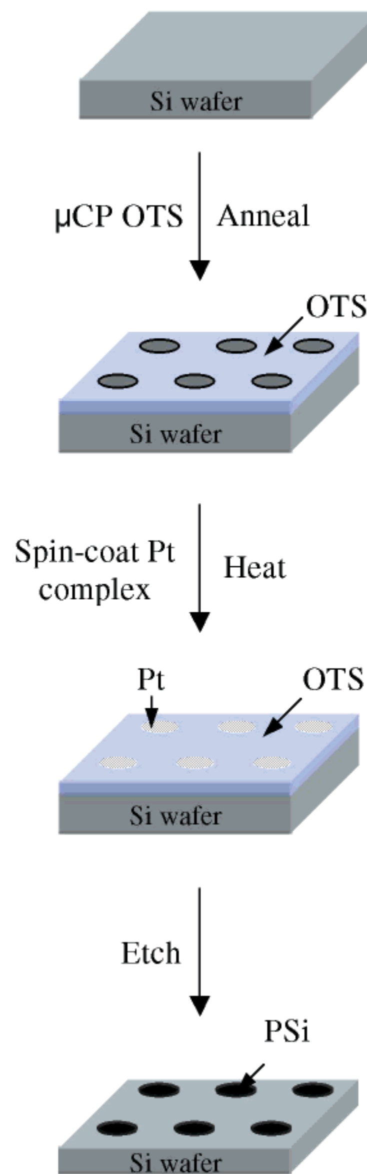

[a] OTS is microcontact printed on a Si substrate, followed by Pt deposition. The Pt complex assembles in the regions of the substrate not covered with OTS. The substrate is heated to remove the solvent and form Pt colloids. Porous silicon forms in the Pt-coated areas when the sample is etched with EtOH/HF (49%)/H_2O_2 (30%).

(34) Finnie, K. R.; Haasch, R.; Nuzzo, R. G. *Langmuir* **2000**, *16*, 6968−6976.

(35) Stein, J.; Lewis, L. N.; Gao, Y.; Scott, R. A. *J. Am. Chem. Soc.* **1999**, *121*, 3693−3703.

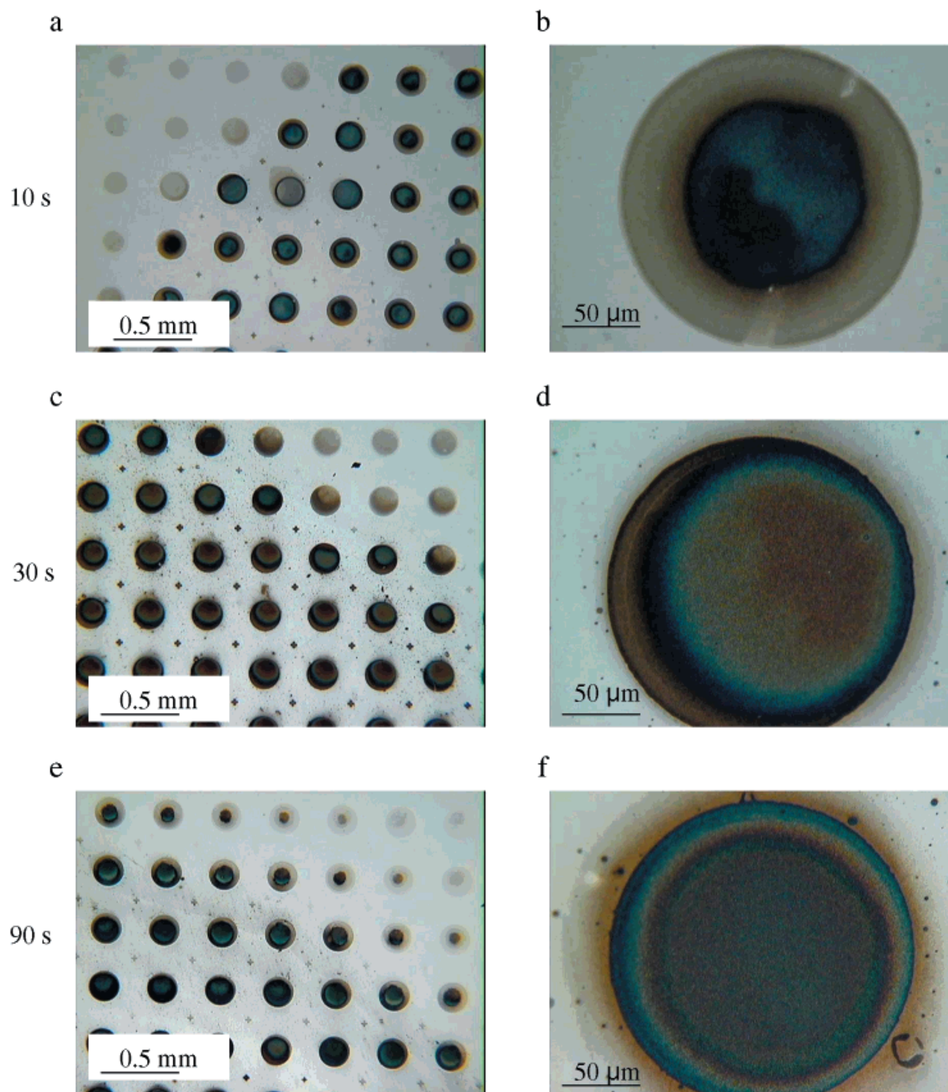

Figure 1. Optical micrographs of patterned samples etched with a 50-μL drop of the etchant for (a) 10, (b) 10, (c) 30, (d) 30, (e), and (f) 90 s. The images at a lower magnification show both etched and unetched areas. The higher magnification images on the right are taken from near the center of the etched area.

for an equivalent time. These observations demonstrate that the μCP patterned self-assembled monolayer (SAM) is an effective resist for orthogonally patterning the Pt(0) complex catalyst and that the species derived from it are necessary agents for the etching process. The composition of the etchant is also a crucial process control parameter. We noted, for example, that etching a Pt-coated sample in a 1:1 mixture of EtOH/HF (49%) for 5 min produced only a slight color change, while etching in H_2O_2 (30%) alone produced no noticeable change over this same time.

Characterization of Etched Pixels Using Scanning Electron Microscopy. An SEM image taken of a sample before etching shows the fidelity of the patterned OTS-SAM transferred by μCP. The micrograph shown in Figure 2a is a Si sample modified by the OTS-SAM, but prior to deposition of the Pt(0) complex. The image contrast results from differences in the secondary electron emission due to the presence of the SAM. The image shown in Figure 2b corresponds to the sample after deposition of the Pt(0) complex and immersion in the etching solution. The etching step produces gross structural changes in the non-OTS-bearing regions of the sample, with the changes effected by a 30-s etch inverting the image contrast seen in the initial SEM micrograph (Figure 2b). As in the optical micrographs, a radially symmertric variation in morphology is observed in the SEM images of the etched pixels, again indicating that the porous silicon morphologies depend on the location within the dot. The high-resolution SEM images shown in Figure 3 were taken from the area in the center of the circular pixels, the regions where the etching appears to initiate. The data shown in Figure 3 clearly demonstrate that this etching generates nanoscale (porous) structures in the pixel domains. As is seen in the side views of cleaved samples (Figure 3a, c, e), the pore depths of the pixels increase with the etch time. Pores were obtained with no specific orientation relative to the underlying substrate crystal structure. The sample etched for 10 s has a very thin layer of porous silicon, one whose morphology is not well defined. At 30 s, the layer generated is ∼200 nm thick, and there are features composed of small structures of <30 nm in size. At 90 s, the etching produced porous layers that are more than 450 nm thick. Interestingly, the pore sizes generated vary nonlinearly with the etching time, reaching a limiting structure under the conditions examined here of granular textures of <50 nm in size. The regions outside of the OTS-defined pixels are much smoother for all of the etch times investigated.

Luminescence Properties of Patterned Porous Silicon Samples. Under a UV lamp, the patterned porous silicon

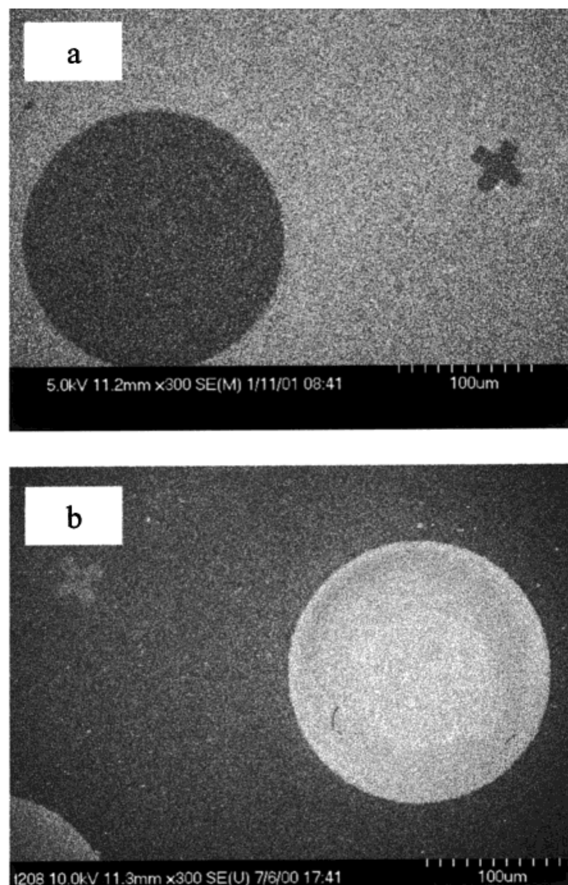

Figure 2. SEM images of an OTS-coated sample (a) before etching and (b) after etching with a 50-μL drop of etchant for 30 s.

samples emit an intense orange light that is easily visible to the naked eye. This is a very striking result given the limited fill factor of the pixels in this array design. More importantly, though, we found that this photoluminescent property is remarkably stable, being maintained even after weeks of exposure to air. The emission patterns, seen in a sample etched for 30 s, are shown in the fluorescence micrograph presented in Figure 4a. The dimensions of the features seen in this image correlate closely with those of the contact-printed OTS pattern. It is notable that the spreading of the brown color seen in the optical micrographs is not seen in the fluorescence image, suggesting a low quantum yield for emission in these regions. An emission spectrum of a patterned sample etched for 30 s was collected at $\lambda_{ex} = 350$ nm (Figure 4b) and shows a broad emission band centered around 580 nm. Since the slit was fixed at 3 mm, the recorded spectrum is of multiple dots and crosses.

Imaging Secondary Ion Mass Spectrometry. SIMS images were recorded to show the secondary ion distributions of Pt and Si on samples before and after etching. These images are shown in Supporting Information. Before etching, the Pt signal is very intense at the center of the pixel, and a ~4-fold gradient in Pt is clearly evidenced. After etching, the spatial distribution of the Pt concentration remains similar to that seen before etching, but the gradient is reduced to ~2-fold. The Si distribution before etching is uniform throughout the image field. There is a distinct separation seen between areas of high- and low-Si signal intensity after etching for 30 s, however. At an etching time of 60 s, the Si-deficient spot grows larger, essentially covering all of the circular pixel area. The low-Si signal level seen in the dark area arises from the low density of the porous silicon layer. Notably, the region of low-Si signal intensity coincided with the region of high Pt content. In addition to Pt and Si, SIMS maps of C and O were also obtained (data not shown). The C signal before etching was found to be somewhat higher in the regions lying outside of a pixel, a verification that the OTS was printed with good pattern fidelity.

Scanning Auger Spectroscopy. Auger line scans of a representative pixel before etching (Figure 5a and b) were obtained for C (272 eV), O (510 eV), Si (1621 eV), and Pt (64 eV) Auger transitions. A corresponding SEM mode image of the pixel is shown in Figure 5c. An expanded view of the Pt line scan is shown in Figure 5b. The atomic concentrations measured in these data establish several structural trends. First, Pt is present only in the pixel and only then in relatively small amounts. The mass coverage of the Pt is highest in the center of the pixel. The pattern of the C line scans is complex and suggests contributions from both the OTS (outside the pixel) and carbonaceous species associated with the Pt complex generated by the surface treatment. The Pt colloids generated by the surface treatment (see below) are expected to bind carbonaceous materials strongly at their surfaces. The modulation of the apparent O concentrations in an annular ring at the boundary of the pixel appears to mirror the compositional heterogeneity suggested by the SIMS data. This annular distribution (one that is too large to be completely ascribed to the effects of attenuating overlayers on electrons with modest mean free paths) is amplified during the etching. Finally, the contrast seen in the SEM image reflects the heterogeneity of the secondary electron emission across the sample. The samples themselves have very little height contrast at this resolution. The image thus correlates with the compositional maps described above.

X-ray Photoelectron Spectroscopy. XPS data were obtained in two ways. The survey spectra shown in Figure 6 were measured on samples that had not been patterned with OTS. Rather, in this case, the sample was treated uniformly with the Pt(0) complex and subsequently processed in a manner that was otherwise identical to that used on patterned samples. A portion of this sample was then treated with etchant solution for 60 s, and the XPS data were then measured in both the unetched (Figure 6a) and etched (Figure 6b) regions. The data clearly show that submonolayer quantities of Pt are present on the unetched samples as judged by the presence of the Pt 4f core level peaks near 74 eV. The quantity of Pt present in spectra measured in the etched region of the sample is much lower.

Etching also produces a marked decrease in the O 1s (~533 eV) and C 1s (285 eV) core level intensities relative to those of Si (e.g., the Si 2s ~153 eV and Si 2p ~100 eV). Both spectra show relatively low levels of F as judged by the F 1s core level seen around 688 eV. The presence of F in the unetched region of the sample likely results from vapor-phase transport of HF from the solution used to etch the other half of the wafer. The data suggest that the etchant must leave a high density of hydrogen-passivated sites in order to account for the low densities of fluoride- or oxide-terminated species on the porous surface of the etched sample. High-resolution scans of the Pt $4f_{7/2}$ core levels (Supporting Information) reveal the presence of two different oxidation states for the Pt present on the unetched regions of the sample (Pt $4f_{7/2}$ at 71.6 and 73.1 eV). The dominant low-binding energy components are consistent with the presence of metallic clusters. The Pt $4f_{7/2}$ peaks near 73 eV are consistent with the presence of Pt(II) species.[35]

High-resolution scans of the Si 2p core levels are shown in Supporting Information. Data measured in unetched areas are dominated by an elemental Si peak at 99.8 eV; lesser contributions are also seen at 101.0 (suboxide) and 103.0 eV (SiO_2).

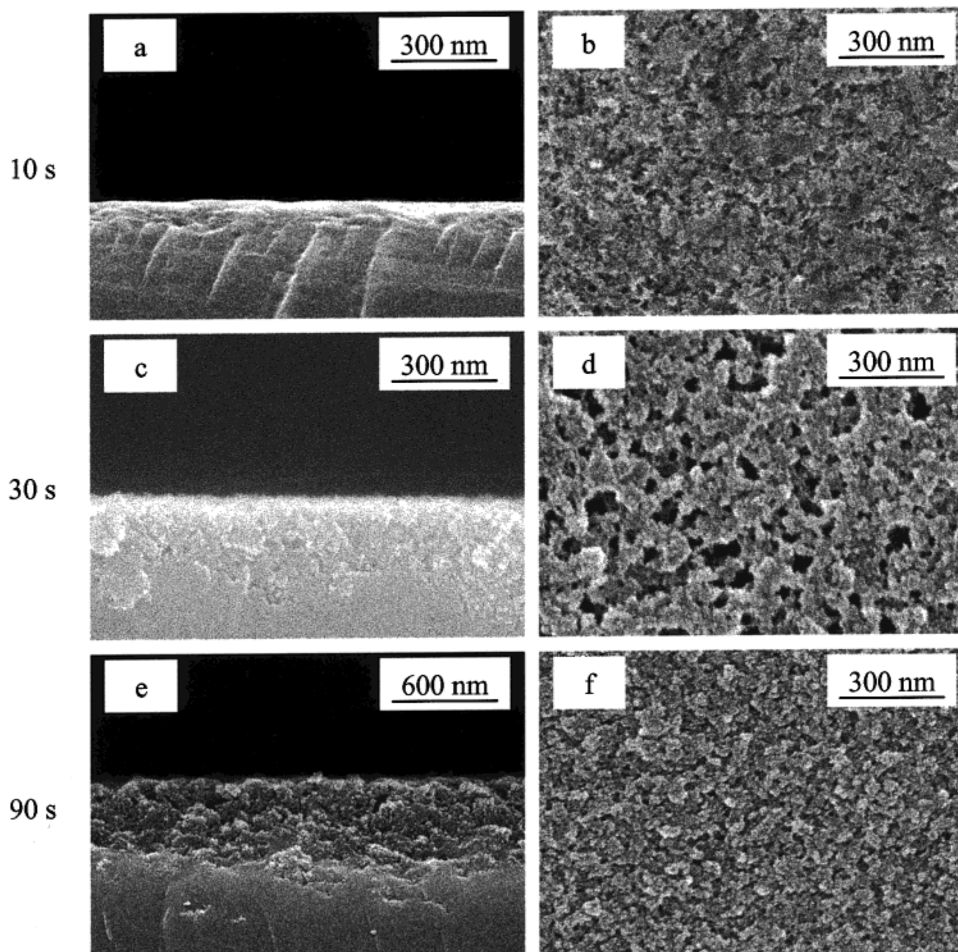

Figure 3. SEM images of etched samples showing cross-sectional (left) and top (right) views of the pixels. The samples were etched with a 50-μL drop of etchant for (a) 10, (b) 10, (c) 30, (d) 30, (e) 90, and (f) 90 s. The porous silicon film is hardly apparent in (a), ~200 nm thick in (c), and >450 nm thick in (e).

We note that the Pt(0) complex used in the patterning contains siloxane linkages in the ligand system used to stabilize the metal center. The processing used in the patterning does appear to lead to the decomposition of the complex, but it is unclear whether fragments of the ligands are retained at the surface. Since siloxane moieties are expected to have 2p binding energies in the range of ~101 eV,[36,37] the data suggest that such species are retained. On an OTS-patterned sample, such species must be present in the regions associated with the orthogonal resist layer. It is known, though, that the suboxide of Si can also show binding energies in this region,[38] so some care must be used in interpreting the Si 2p XPS data. In a sample exposed to the etchant, only one Si 2p core level peak is seen (centered at 100.0 eV). The small sizes of the Si features generated by etching are likely to lead to significant perturbations of the Si 2p binding energies due to both the consequences of band bending and the influence of cluster size on the final state contributions to the core level binding energy. For these reasons, we do not assign the Si 2p peak in the etched area to a specific chemical form of Si.

In a second XPS study, the Pt $4f_{7/2}$ and C 1s core levels of an unetched sample were imaged. These data, shown in Figure 7, demonstrate the successful orthogonal deposition of Pt into the circular regions defined by the OTS pattern. A high-magnification Pt $4f_{7/2}$ image (see Supporting Information) showed a clear gradient distribution of the Pt centers within the pixel. The image shown in Figure 7 is a cross-correlated Pt $4f_{7/2}$ and C 1s image map, here recorded at a lower magnification. The pixel hues in this latter image illustrate the orthogonal patterning contrasts imposed by the OTS templates. The mass of the Pt in the cross-shaped fiduciary markers is too low to be observed by this XPS imaging experiment. A survey spectrum of a 40-μm spot centered on the pixel has a Pt $4f_{7/2}$ binding energy of 74 eV. The Pt $4f_{7/2}$ intensity in a spectrum of a 40-μm spot measured off the pixel was too small to observe above the background counting rate.

Discussion

Pt-Assisted Etching of Silicon with HF/H_2O_2. Taken together, these data establish the viability of soft lithographic patterning methods, in particular the orthogonal deposition of zerovalent Pt complexes on OTS-patterned surfaces mediated by μCP, as a means of generating porous silicon microstructures. Although this work did not establish the ultimate design rules that might be reached with these methods, it does illustrate that feature sizes of interest for bioanalytical applications[39-41] (i.e.,

(36) Chan, V. Z.-H.; Thomas, E. L.; Frommer, J.; Sampson, D.; Campbell, R.; Miller, D.; Hawker, C.; Lee, V.; Miller, R. D. *Chem. Mater.* **1998**, *10*, 3895−3901.

(37) Ouyang, M.; Yuan, C.; Muisener, R. J.; Boulares, A.; Koberstein, J. T. *Chem. Mater.* **2000**, *12*, 1591−1596.

(38) Grunthaner, P. J.; Hecht, M. H.; Grunthaner, F. J.; Johnson, N. M. *J. Appl. Phys.* **1987**, *61*, 629−638.

(39) Singhvi, R.; Kumar, A.; Lopez, G. P.; Stephanopoulos, G. N.; Wang, D. I. C.; Whitesides, G. M.; Ingber, D. E. *Science* **1994**, *264*, 696−698.

(40) St. John, P. M.; Davis, R.; Cady, N.; Czajka, J.; Batt, C. A.; Craighead, H. G. *Anal. Chem.* **1998**, *70*, 1108−1111.

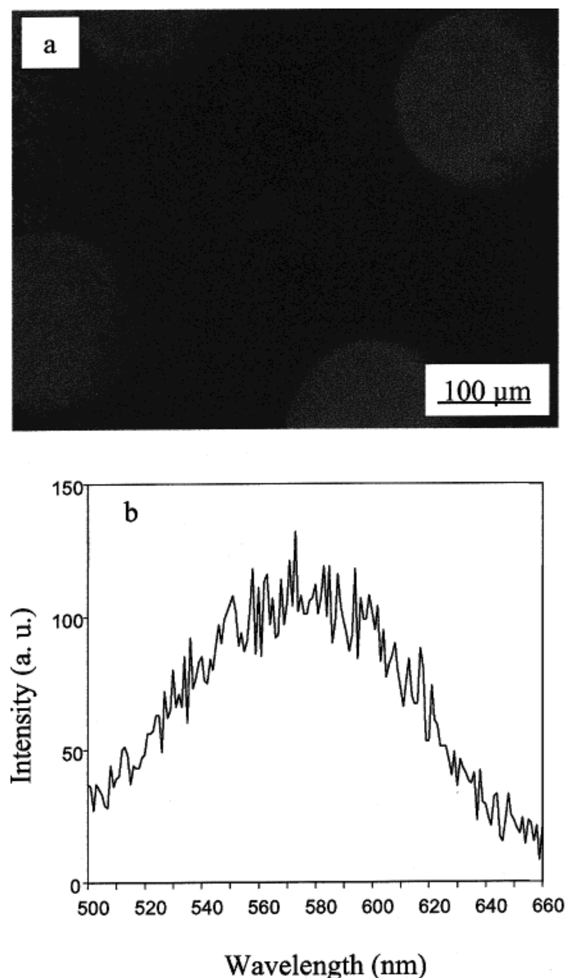

Figure 4. (a) Fluorescence micrograph recorded using a 360-nm excitation source, and (b) emission spectrum recorded at 350 nm using a 3-mm slit. In both cases, patterned samples etched for 30 s with a 50-μL drop of etchant were used.

in the >10-μm size range) can be generated easily. Higher resolution features appear to be within the reach of these methods, and given proper mask design and etching conditions, spatial resolution should be limited only by the nature of the local corrosion cells created by the Pt-mediated wet etching. The etching mechanism has not been completely established, but some aspects of it are understood from the earlier work of Li and Bohn. They proposed a mechanism for the Pt-assisted etching of Si as follows:[13]

Cathode (Pt)

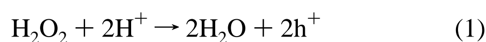

$$H_2O_2 + 2H^+ \rightarrow 2H_2O + 2h^+ \quad (1)$$

$$2H^+ \rightarrow H_2 + 2h^+ \quad (2)$$

Anode (Si)

$$Si + 4h^+ + 4HF \rightarrow SiF_4 + 4H^+ \quad (3)$$

$$SiF_4 + 2HF \rightarrow H_2SiF_6 \quad (4)$$

Overall

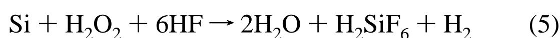

$$Si + H_2O_2 + 6HF \rightarrow 2H_2O + H_2SiF_6 + H_2 \quad (5)$$

This chemically directed etching displays properties expected for a pitting corrosion process. The oxidation of Si at the local anode is facilitated by holes (h^+) generated by the decomposition of H_2O_2 at a local Pt cathode. A sufficient amount of h^+ must be supplied by the oxidizing agent in order to maintain the etching at a reasonably fast rate. The Pt species generated by the μCP patterning appear to be remarkably efficient toward this end, mediating etch rates much greater than those obtained for sputtered Au or Au/Pd alloys.[13] The acceleration in etch rate has led these investigators to speculate that Pt may act catalytically with respect to reaction 1, reaction 2, or both. The sensitivity to local corrosion is confined to the Pt(0)-containing areas, which provides a useful contrast to conventional stain etching with HF/HNO_3 solutions (vis-à-vis facilitating the ease of patterning porous silicon). The SIMS images (and other data) clearly demonstrate that the areas with high Pt concentrations are etched preferentially; holes thus generate useful chemical reactions only in the local vicinity of the metal. This behavior contrasts that seen for metal patterns deposited by sputtering (and other deposition techniques that leave the uncoated areas

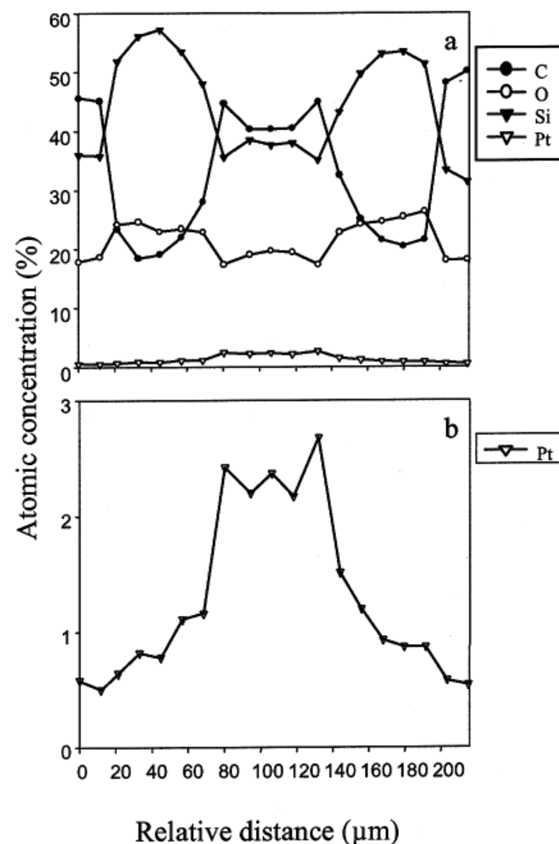

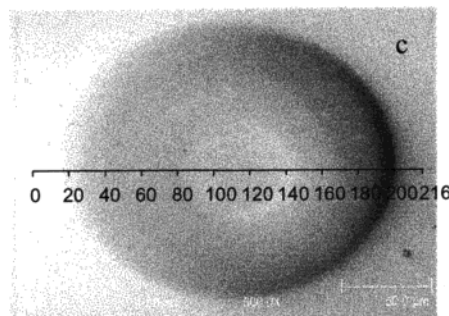

Figure 5. Auger area scans of a Pt-patterned sample before etch. (a) Relative atomic concentrations (%) of C (•), O (○), Si (▼), and Pt (∇) are plotted as functions of relative distance across a pixel; (b) expanded plot of Pt atomic concentration relative to the other three elements; (c) SEM image of the scanned area with a scale that corresponds to the *x*-axis of (a) and (b).

(41) Mayne, A. H.; Bayliss, S. C.; Barr, P.; Tobin, M.; Buckberry, L. D. *Phys. Status Solidi A* **2000**, *182*, 505−513.

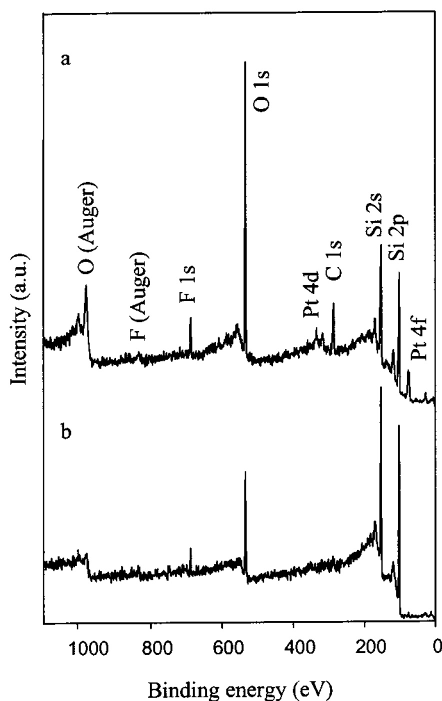

Figure 6. XPS survey spectra of a Pt-coated sample after it was etched with a 50-μL drop of etchant for 60 s. (a) Outside the etched area; (b) inside the etched area.

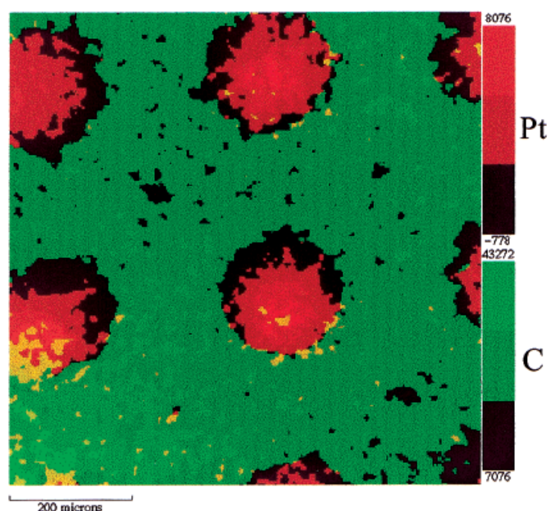

Figure 7. Cross-correlated, low-magnification XPS image measured for the Pt $4f_{7/2}$ (shown in red) and C 1s (shown in green) core levels measured at 74 and 285 eV, respectively.

bare). Hole transport in the latter case can lead to etching hundreds of micrometers distant from the metal pattern. The presence of OTS as an orthogonal resist in this μCP technique effectively confines etching to only the desired areas, since reactants in the anode reactions 3 and 4 cannot gain access to the Si surface.

We know that the Pt is deposited initially on the surface of the sample and that even at the outset of etching its coverage is very low. We do not know whether a significant portion of the Pt content is lost from the surface as the etching proceeds. The XPS analysis of an etched sample clearly indicates a substantial decrease in the Pt concentration within the XPS sample depth, a result that can be related either to the loss of Pt to the solution or to attenuation of the photoelectrons arising from Pt species burrowing into the pores of the evolving porous silicon structures. The SIMS Pt image maps tend to support the latter possibility as being a contributor to this etching process. The nature of the catalytic Pt centers is an additional point of interest to consider in the context of the mechanisms that lead to the microstructures seen. The XPS data clearly suggest that the printing leads to the formation of Pt species that exhibit at least some metallic character. Nanoscale clusters are most likely the products of this deposition, although independent data from microscopy has yet to establish this point definitively. It also appears that, as the etching proceeds, these species decompose, leaving behind Pt in a higher oxidation state.

The progress of the etching is conveniently monitored by the changes seen in the Si 2p core levels. Prior to etching, the Si 2p spectrum reveals the presence of elemental Si and native oxide (siloxane, suboxide, SiO_2) within the XPS sample depth. The etchant does appear to effect at least a partial stripping of the oxide from the affected region.

The structure of the porous silicon films formed by the soft lithographic patterning method described here resembles that of samples prepared by stain etching or anodization of lightly doped p-Si wafers.[10,11] The SEM images of the etched samples exhibit rough porous silicon microstructures with randomly connected and finely distributed pores. The bottom of the film, as viewed in cross-sectional SEM micrographs, is not smooth, but the overall film thickness is uniform. In contrast to other reported methodologies,[10,11,42] there does not appear to be a structurally distinct layer that forms between the porous silicon film and the substrate. Rather, the bulk crystal appears more generally terminated in the dense pore structure of the etched silicon layer (as has been noted to be the case for certain anodic etching processes of lightly doped p-type Si).[43]

The exact morphology of the porous silicon depends heavily on the location within the Pt-modified pixel, most likely because a radial gradient of Pt concentration exists within each pixel. The microscopy data provide evidence that the etching is most extensive where the Pt concentration is highest, with film thickness reaching >450 nm in 90 s at the center of the pixels. There is no correlation between the porous silicon structure and the gradient of etching depth measured across the pixel, however.

The stable porous silicon patterns produced in this work were derived from a microcontact printed OTS pattern containing circles ~150 μm in diameter and crosses whose smallest dimension is ~10 μm. Photoluminescence from an ensemble of these patterned dots was easily observable at room temperature, with the measured emission peak centered at ~580 nm. The spectrum itself is quite broad, further suggesting the response is due to a weighted heterogeneous ensemble of nanostructures. One finds in the micrographs of the porous silicon structures generated an interesting point of contrast for this latter observation. The photoluminescent properties of porous silicon are believed to arise from the effects of quantum confinement. The sizes of the structures associated with emission in the 580-nm range are expected to be of the order of 10 Å on average.[44] The majority of structures seen in the SEM cross-sectional micrographs appear to be larger than this. The dominant feature seen in the micrograph, however, need not be those with the highest quantum yields. This emphasizes the point that considerable caution must be used when structural data are correlated with the optical properties derived from an ensemble measurement of the sample.

(42) Beale, M. I. J.; Chew, N. G.; Uren, M. J.; Cullis, A. G.; Benjamin, J. D. *Appl. Phys. Lett.* **1985**, *46*, 86−88.

(43) *Properties of Porous Silicon:* Canham, L. T., Ed.; EMIS Datareviews Series 18; INSPEC: London, 1997.

We now consider the factors that might serve to limit the fidelity of the pattern formation. The microscopy data indicate that etching is initially restricted to the Pt-coated areas of the substrate, but spreads to areas surrounding the pixels at longer etching times. This spreading is caused by several factors. Undoubtedly, the quality of patterned porous silicon formation is most strongly influenced by the fidelity of the orthogonal Pt patterning. Selective deposition of the Pt in the OTS-free areas of a patterned substrate was confirmed by the XPS, Auger, and SIMS data, which indicate that OTS is an effective resist for this aspect of the patterning. However, the OTS resist on the outside of the pixels fails shortly after it comes in contact with the etchant ($t \geq 30$ s), making the substrate prone to etchant attack. The degradation of pattern fidelity can occur either due to Pt migration or to hole transport after carrier injection (reactions 1 and 2). Although we cannot rule out Pt migration, previous experiments demonstrated that etching could be observed on the back (not Pt-coated) side of a 200-μm-thick Si wafer with Pt sputter coated on the front.[45] Only h^+ transport can explain this observation. Whether the spreading of the pattern is caused by the migration of Pt or h^+ transport, rogue etching occurs most severely in the vicinity of the Pt-coated areas.

These observations suggest that an important issue regarding the pattern transfer therefore resides in the μCP of the OTS layer. This step determines the fidelity of the Pt transfer, the ultimate etch resistance of the unmodified substrate, the current density it can carry as a cathode, and the densities of the defects that allow Pt deposition in undesired parts of the sample. In addition, the patterning of OTS via μCP is subject to reactive spreading, which in turn reduces the lateral dimensions of the features transferred.[46] We therefore believe that the orthogonal patterning abilities of the passivating layer can be improved by switching from OTS to a longer alkyltrichlorosilane ink (e.g., docosyltrichlorosilane, DTS). Such inks have recently been shown to have more desirable characteristics than OTS in terms of pattern spreading and durability toward wet chemical etching.[34]

Finally, we note that the homogeneity of the Pt content within a given pixel is not easily controlled, since the Pt complex is spun-on, allowing the Pt particles to nucleate and concentrate in regions under the bias of the wetting and evaporation properties of the ink solvents. A more direct ligand design that mediates the Pt binding to the substrate, or the additive direct patterning of the catalyst itself, should serve to address this problem. Such limitations notwithstanding, these structures should still be of great utility for applications in chemical sensing and spectrometry, especially those that would benefit from significantly simplified production methods. We will develop these themes further in forthcoming publications.

Acknowledgment. This work was supported by DARPA (N66001-98-1-8915), the Department of Energy (DEFG02-96ER45439), and the National Science Foundation (CHE-9626871). Surface analyses were carried out at the Center for Microanalysis of Materials, University of Illinois, which is supported by the Department of Energy under Contract DEFG02-96ER45439.

Supporting Information Available: Selected figures discussed in text. This material is available free of charge via the Internet at http://pubs.acs.org.

JA010367J

(44) Schuppler, S.; Friedman, S. L.; Marcus, M. A.; Adler, D. L.; Xie, Y.-H.; Ross, F. M.; Chabal, Y. J.; Harris, T. D.; Brus, L. E.; Brown, W. L.; Chaban, E. E.; Szajowski, P. F.; Christman, S. B.; Citrin, P. H. *Phys. Rev. B* **1995**, *52*, 4910−4925.

(45) Chattopadhyay, S.; Li, X.; Bohn, P. W. Unpublished results.

(46) Jeon, N. L.; Finnie, K.; Branshaw, K.; Nuzzo, R. G. *Langmuir* **1997**, *13*, 3382−3391.